Research Article
Modeling of Coupled Roll and Yaw Damping of a Floating Body in Waves

S. K. Das and S. N. Das

A mathematical model is described to investigate the damping moment of weakly nonlinear roll and yaw motions of a floating body in time domain under the action of sinusoidal waves. The mathematical formulation for added mass moment of inertia and damping is presented by approximating time-dependent coefficients and forcing moments when small distortion holds. Using perturbation technique, we obtain orderwise equations wherein the closed-form solution is obtained for zeroth-order case, and for higher-order cases we resort to numerical integration using Runge-Kutta method with adaptive step-size algorithm. In order to analyze the model result, we perform numerical experiment for a vessel of 19190 tons under the beam wave of 1 m height and frequency 0.74 rad/s. Closer inspection in damping analysis reveals that viscous effect becomes significant for roll damping; whereas for yaw damping, contribution from added mass variation becomes significant.

1. Introduction

Understanding of roll and associated damping is important for the safety of a ship. Considerable attention has been paid by various researchers to investigate roll-damping moment since the pioneering work of Froude [1]. The oldest roll-damping formulation of Froude was based on linear-plus-quadratic velocity-dependent form to account for energy dissipation mechanism during roll motion. The important research work carried out in this direction during last century can be obtained from Kerwin [2], Haddara [3], Dalzell [4], Haddara [5], and Nayfeh and Khdeir [6]. Haddara [3] first introduced the linear-plus-cubic velocity-dependent roll-damping moment to improve analytical model arising from the classical linear-plus-quadratic form. Dalzell [4] performed a detailed

study on the cubic and quadratic models by using the method of slowly varying parameters and a least-square technique. Haddara [5] further suggested different roll-damping models by using the same roll decay data. A stochastic version of Haddara's technique was adopted later by Dalzell [4] to investigate various models. Though this method is accurate and included angle-dependent forms, yet it could not separate the influence of the angle-dependent components of the same order of magnitude. Cardo et al. [7] introduced two types of damping moments containing linear-quadratic and linear-cubic forms in the angular velocity of rolling equation. Mathisen and Price [8] identified the roll-damping parameters by perturbation technique. Spouge [9] compared various methods for the analysis of forced roll and roll decrement experiments in calm water from which nonlinear roll-damping coefficients may be determined. Roberts [10] related the roll-damping moment to a loss function using a stochastic approach. His analysis estimates nonlinear damping by using a cubic spline interpolation of peak amplitudes. Bass and Haddara [11] separated the influence of all the different components of the roll-damping moment through energy approach, which provide an insight into the damping mechanism. Haddara and Bennett [12] studied the angular dependence roll damping by using experimentally obtained free roll decay curves for an R-class icebreaker model and an arctic-class cargo model. Haddara and Bass [13] also investigated the form of roll-damping moment for small fishing vessels to gain better understanding of the energy dissipating mechanism for these vessels. Chun et al. [14] investigated the roll-damping characteristics of a 3-ton class fishing vessel experimentally and numerically.

In the present work, we propose a new form of damping moment for coupled roll and yaw motions of a floating body which is excited by unidirectional sinusoidal wave. The nonlinearity in roll damping is realized by considering the variation of added mass in the damping moment formulation and also analyzing (i) the change in time-dependent virtual mass, (ii) linear roll angle, (iii) quadratic roll angle, and (iv) viscous effects. Using perturbation technique, we derive zeroth-order and other higher-order equations, wherein for zeroth-order solution we adopt the procedure described by Das and Das [15] and Salvesen et al. [16] to obtain integrated sectional added mass and damping over the length of the body. We seek analytical solution in time domain by applying Laplace transform technique for a given frequency. For higher-order perturbed equations, an adaptive Runge-Kutta method with step-size adjustment algorithm is employed to reveal damping characteristics for coupled system.

2. Mathematical formulation

Usually, frequency response analysis corresponding to a Fourier approach can be conveniently applied in ship motion studies [17]. Owing to complex interactions between the hull- and ship-generated waves, the governing equations are represented in the form of integrodifferential equations, posing enormous difficulty in solving [18]. Such difficulty can be conveniently avoided by considering the ship motion in regular waves. This reduces the integrodifferential equation into ordinary differential equation with coefficients corresponding to the frequency of the encountering wave. We consider a Cartesian coordinate system (x, y, z) fixed with respect to the mean position of the ship with z-axis acting in the vertical upward direction. In Figure 2.1, the motion responses represented
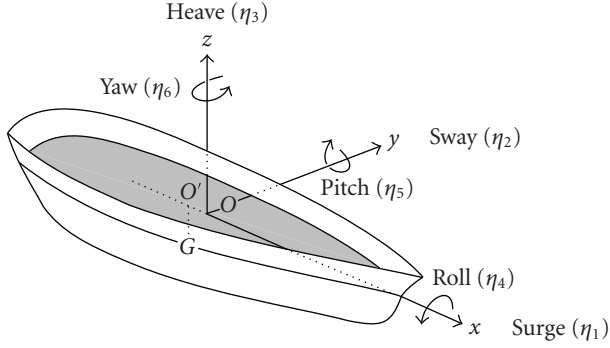
Figure 2.1. Motion definition of a floating body.

by η_1, η_2, η_3, η_4, η_5, and η_6 indicate surge, sway, heave, roll, pitch, and yaw, respectively. Following the approach suggested by Tick [17] for linearly coupled system in two degrees of freedom, one can obtain

$$\sum_{k=4,6} \left[-\omega^2 M_{jk}(\omega)X_k(\omega)e^{i\omega t} + i\omega B_{jk}(\omega)X_k(\omega)e^{i\omega t} + C_{jk}(\omega)X_k(\omega)e^{i\omega t} \right]$$
$$= D_j(\omega)F(\omega)e^{i\omega t}, \quad j = 4,6, \tag{2.1}$$

where $X_k(\omega)$ is the displacement, $F(\omega)$ is the wave force with amplitude $D_j(\omega)$, $M_{jk}(\omega)$, $B_{jk}(\omega)$, and $C_{jk}(\omega)$ are the frequency-dependent virtual mass, damping, and restoring coefficients, respectively. Defining

$$\eta_k(t) = X_k(\omega)e^{i\omega t}, \quad f(t) = F(\omega)e^{i\omega t}, \quad k = 4,6, \tag{2.2}$$

we obtain

$$\sum_{k=4,6} \left[M_{jk}(\omega)\ddot{\eta}_k(t) + B_{jk}(\omega)\dot{\eta}_k(t) + C_{jk}(\omega)\eta_k(t) \right] = D_j(\omega)f(t), \quad j = 4,6. \tag{2.3}$$

Equation (2.3) provides time-dependent formulation of motion response expressed as ordinary differential equation. It is apparent that the motion variables (η_i), exciting force $f(t)$, and wave frequency (ω) described in (2.3) are complex quantities and can be expressed as algebraic sum of real and imaginary parts. Accordingly, the forcing function $f(t)$ becomes

$$f(t) = F(\omega)e^{i(\omega_R + i\omega_I)t} = F(\omega)e^{i\omega_R t}e^{-\omega_I t}. \tag{2.4}$$

For simplicity, we assume the imaginary part of wave frequency (ω_I) is equal to zero, yielding

$$f(t) = F(\omega)e^{i\omega_R t}. \tag{2.5}$$

The motion responses and forcing functions are sum of real and imaginary parts,

$$\eta_j = \eta_{jR} + \eta_{jI}, \quad F_j = F_{jR} + F_{jI}, \quad j = 4,6. \tag{2.6}$$

Considering only the real part of motion response and exciting moment for a given wave frequency, the equation of motion for coupled roll and yaw can be described using the notation of operator [19] as

$$[d_{i4}\eta_4(t) + d_{i6}\eta_6(t)] = F_i(t), \quad i = 4,6, \tag{2.7}$$

where the operator d_{ij} is given by

$$d_{ij} = \Delta_{ij}(t)\frac{d^2}{dt^2} + B_{ij}(t)\frac{d}{dt} + C_{ij}(t), \quad i,j = 4,6, \tag{2.8}$$

$F_i(t)$, $i = 4,6$, are the exciting wave moments, $\Delta_{ij}(t) = M_{ij} + A_{ij}(t)$ is the virtual mass moment of inertia, $A_{ij}(t)$, $B_{ij}(t)$, and $C_{ij}(t)$ are the cross-coupled coefficients like added mass, damping, and restoring in the direction i due to any motion in the direction j. Using (2.7) and (2.8), the governing equation can be written in time domain as [20]

$$\{[M_{ij}] + [A_{ij}(t)]\}[\ddot{\eta}_i] + [B_{ij}(t)][\dot{\eta}_i] + [C_{ij}(t)][\eta_i] = [F_j(t)]. \tag{2.9}$$

The coefficient matrices can be expressed as

$$
[M_{ij}] = \begin{bmatrix} I_4 & -I_{46} \\ -I_{64} & I_6 \end{bmatrix}, \qquad [A_{ij}(t)] = \begin{bmatrix} A_{44}(t) & A_{46}(t) \\ A_{64}(t) & A_{66}(t) \end{bmatrix},
$$
$$
[B_{ij}(t)] = \begin{bmatrix} B_{44}(t) & B_{46}(t) \\ B_{64}(t) & B_{66}(t) \end{bmatrix}, \qquad [C_{ij}(t)] = \begin{bmatrix} C_{44}(t) & 0 \\ 0 & 0 \end{bmatrix},
$$
$$
[\ddot{\eta}_i] = \begin{bmatrix} \ddot{\eta}_4 \\ \ddot{\eta}_6 \end{bmatrix}, \qquad [\dot{\eta}_i] = \begin{bmatrix} \dot{\eta}_4 \\ \dot{\eta}_6 \end{bmatrix}, \tag{2.10}
$$
$$
[\eta_i] = \begin{bmatrix} \eta_4 \\ \eta_6 \end{bmatrix}, \qquad [F_i(t)] = \begin{bmatrix} F_4(t) \\ F_6(t) \end{bmatrix},
$$

where the components in the matrices $[\dot{\eta}_i]$ and $[\ddot{\eta}_i]$ indicate time derivatives. Introducing dimensionless analysis (given in the appendix (A.1)) and substituting (2.10) in (2.9), and after dropping the bars, we obtain

$$a_1(t)\ddot{\eta}_4 + a_2(t)\dot{\eta}_4 + a_3(t)\eta_4 + b_1(t)\ddot{\eta}_6 + b_2(t)\dot{\eta}_6 = F_4(t), \tag{2.11}$$
$$a_4(t)\ddot{\eta}_4 + a_5(t)\dot{\eta}_4 + b_3(t)\ddot{\eta}_6 + b_4(t)\dot{\eta}_6 = F_6(t). \tag{2.12}$$

The coefficients $\{(a_1(t),a_4(t));(a_2(t),a_5(t))\}$ and $\{(b_1(t),b_3(t));(b_2(t),b_4(t))\}$ represent the time-dependent virtual mass moment of inertia and damping moments for roll and yaw, respectively and $a_3(t)$ is the roll restoring moment. $F_4(t)$ and $F_6(t)$ are the forcing moments for roll and yaw. I_j is the moment of inertia in the jth mode, and I_{jk} is the product of inertia.

3. Approximation of hydrodynamic coefficients and forcing moments

As waves pass through any floating body, the mass moment of inertia of the displaced volume of water may undergo changes with time. Hence, the virtual mass moment of inertia and the damping coefficients are assumed to vary with time [19]. We approximate these coefficients by using series expansions where the nonlinearity is weak but the assumption of small distortion still holds. Accordingly, the added mass terms appearing in (2.11) and (2.12) are expressed in generalized vector form as

$$\{\chi(t)\} = \sum_{i=0}^{\infty} \varepsilon^i \{\chi_i\}, \tag{3.1}$$

where

$$\{\chi(t)\} = \{a_1, b_1, a_4, b_3\}^T, \qquad \{\chi_i\} = \{a_{1i}, b_{1i}, a_{4i}, b_{3i}\}^T, \quad i = 0, 1, 2, 3, \dots, \tag{3.2}$$

and $\chi_i = \chi_i(t)$ when $i \neq 0$. The superscript T indicates transpose. The series expansion (3.1) is performed with respect to the small dimensionless parameter ε, which is a measure of nonlinearity; arises due to the ratio of roll-damping coefficient (B_{44}) and the product of virtual mass moment of inertia ($I_4 + A_{44}$) and reference wave frequency (ω_0) [13, 14]. As $\varepsilon \to 0$, the hydrodynamic coefficients are no longer nonlinear leading to $\{\chi(t)\} = \{\chi_0\} = \{a_{10}, b_{10}, a_{40}, b_{30}\}^T$; and (3.1) reaches to a fundamental form. The damping coefficients are formulated by considering linear, quadratic, and viscous angular dependencies [20, 21],

$$\psi(t) = \psi_0 + \varepsilon\{\dot{\chi}(t) + \psi_1(t)\,|\eta_k(t)| + \psi_2(t)\eta_k^2(t) + \psi_3(t)\,|\dot{\eta}_k(t)|\}$$
$$+ \varepsilon^2\{\dot{\chi}(t) + \psi_4(t)\,|\eta_k(t)| + \psi_5(t)\eta_k^2(t) + \psi_6(t)\,|\dot{\eta}_k(t)|\} + \cdots, \tag{3.3}$$

where

$$\psi = \{\psi(t)\} = \{a_2, b_2, a_5, b_4\}^T, \qquad \{\psi_i\} = \{a_{2i}, b_{2i}, a_{5i}, b_{4i}\}^T, \quad i = 0, 1, 2, \dots, n, \tag{3.4}$$

and $\varepsilon = B_{44}/(I_4 + A_{44})\omega_0 \ll 1$. Here $\psi_i = \psi_i(t)$ when $i \neq 0$ and (3.3) has been written in generalized form to express the various components of damping coefficients in vector form. The motion variables appearing in the damping coefficient representation (3.3) assume the following form:

$$\eta_k = \{\eta_k\} = \{\eta_4, \eta_6, \eta_4, \eta_6\}. \tag{3.5}$$

The detailed expressions for added mass and damping coefficients ((3.2) and (3.4)) are given in the appendix ((A.2) and (A.3)). As $\varepsilon \to 0$, $\psi(t) \to \psi_0$, representing linear damping case. The roll restoring coefficient $a_3(t)$ arising in (2.11) can be written as

$$a_3(t) = a_{30} + \varepsilon a_{31}(\eta_4) + \varepsilon^2 a_{32}(\eta_4) + \cdots, \tag{3.6}$$

where

$$a_{30} = \rho g \nabla \overline{GM}, \qquad a_{31}(\eta_4) = \kappa_1 \omega^2 \eta_4, \qquad a_{32}(\eta_4) = \kappa_2 \omega^2 \eta_4^3, \tag{3.7}$$

∇ is the displaced volume of the floating body, $\overline{GM}$ is the metacentric height, ρ is the mass density of water, and κ_1, κ_2 are the restoring coefficients for first-order and second-order terms, respectively. For simplicity, we consider roll-restoring coefficient as constant, that is, $\kappa_1 = \kappa_2 = 0$. The external forcing moments $F_i(t)$, $i = 4, 6$, can be approximated as

$$F_i(t) = F_i^0(t) + \varepsilon F_i^1(t) + \varepsilon^2 F_i^2(t) + \cdots , \qquad (3.8)$$

where the zeroth-order term in (3.8) is expressed as

$$F_i^0(t) = F_i^{a0} \operatorname{Sin}(\omega t + \theta), \quad i = 4, 6, \qquad (3.9)$$

F_4^{a0} and F_6^{a0} are the amplitudes of the roll and yaw exciting moments, respectively, θ is the phase angle. The amplitudes of roll and yaw exciting moments for zero forward speed of the body can be expressed in the following form [16]:

$$F_4^{a0} = \alpha\rho \int (f_4 + h_4)\,d\xi, \qquad F_6^{a0} = \alpha\rho \int \xi(f_2 + h_2)\,d\xi, \qquad (3.10)$$

where α is the amplitude of the incident wave with $\theta = 0$, ρ is the density of water, f_i and h_i represent the sectional Froude-Kriloff force and sectional diffraction force, respectively. The integration has been performed over the length of the vessel.

4. Solution procedure

Applying perturbation technique to the nonlinear terms of the angular variables corresponding to roll and yaw [19, 22] yields

$$\eta_k(t) = \eta_{k0}(t) + \varepsilon\eta_{k1}(t) + \varepsilon^2\eta_{k2}(t) + \cdots . \qquad (4.1)$$

Substituting (4.1) and (3.8) to (2.11) and (2.12), and separating the powers of ε, we obtain the orderwise equations for roll and yaw as follows:
  (i) *roll equations*:

$$a_{10}\{\ddot{\eta}_{4i}(t)\} + a_{20}\{\dot{\eta}_{4i}(t)\} + a_{30}\{\eta_{4i}(t)\} + b_{10}\{\ddot{\eta}_{6i}(t)\} + b_{20}\{\dot{\eta}_{6i}(t)\} = \{F_4^i(t)\}, \quad i = 0, 1, 2; \qquad (4.2)$$

  (ii) *yaw equations*:

$$a_{40}\{\ddot{\eta}_{4i}(t)\} + a_{50}\{\dot{\eta}_{4i}(t)\} + b_{30}\{\ddot{\eta}_{6i}(t)\} + b_{40}\{\dot{\eta}_{6i}(t)\} = \{F_6^i(t)\}, \quad i = 0, 1, 2, \qquad (4.3)$$

where $\{\eta_{4i}\} = \{\eta_{40}, \eta_{41}, \eta_{42}\}^T$, $\{\eta_{6i}\} = \{\eta_{60}, \eta_{61}, \eta_{62}\}^T$, $\{F_4^i(t)\} = \{F_4^0(t), F_4^1(t), F_4^2(t)\}^T$, and $\{F_6^i(t)\} = \{F_6^0(t), F_6^1(t), F_6^2(t)\}^T$ for $i = 0, 1, 2$.
    The expression for first-order and second-order forcing functions $F_4^i(t)$ and $F_6^i(t)$ is mentioned in the appendix (A.4).

4.1. Analytical solution. On applying Laplace transform to (4.2) and (4.3), we obtain zeroth-order solution in transformed domain,

$$\overline{\alpha}_i f_{40}(s) + \overline{\beta}_i f_{60}(s) = \overline{\gamma}_i, \quad i = 1, 2, \qquad (4.4)$$

where $f_{40}(s)$ and $f_{60}(s)$ are the angular displacements and $\overline{\alpha}_i$, $\overline{\beta}_i$, and $\overline{\gamma}_i$ are the corresponding coefficients. The detailed solution procedure can be obtained from the investigations of Das and Das [23]. After solving two equations of (4.4), we obtain

$$
\begin{aligned}
f_{40}(s) = \frac{1}{\delta_3} \Bigg[& \frac{c_1^1}{s+\lambda_1} + \frac{c_2^1(s+\varsigma\beta)}{(s+\varsigma\beta)^2 + \left(\beta\sqrt{1-\varsigma^2}\right)^2} + \frac{c_3^1 - c_2^1\varsigma\beta}{(s+\varsigma\beta)^2 + \left(\beta\sqrt{1-\varsigma^2}\right)^2} \\
& + \frac{c_4^1 s}{s^2 + (2\pi\omega)^2} + \frac{c_5^1}{s^2 + (2\pi\omega)^2} \Bigg],
\end{aligned}
$$

$$
\begin{aligned}
f_{60}(s) = \frac{1}{\delta_3} \Bigg[& \frac{c_1^2}{s} + \frac{c_2^2}{s+\lambda_1} + \frac{c_3^2(s+\varsigma\beta)}{(s+\varsigma\beta)^2 + \left(\beta\sqrt{1-\varsigma^2}\right)^2} + \frac{c_4^2 - c_3^2\varsigma\beta}{(s+\varsigma\beta)^2 + \left(\beta\sqrt{1-\varsigma^2}\right)^2} \\
& + \frac{c_5^2 s}{s^2 + (2\pi\omega)^2} + \frac{c_6^2}{s^2 + (2\pi\omega)^2} \Bigg],
\end{aligned}
$$

(4.5)

where ς is the damping factor and β is the undamped natural frequency of the system. c_i^1 and c_j^2 are the unknown coefficients, determined by equating like powers of s resulting in a set of linear algebraic equations. These unknown coefficients were obtained by using Gauss elimination method. The corresponding time-domain solution can be obtained as

$$
\begin{aligned}
\eta_{40}(t) = \frac{1}{\delta_3} \Bigg[& c_1^1 e^{-\lambda_1 t} + c_2^1 e^{-\varsigma\beta t} \cos\left(\beta\sqrt{1-\varsigma^2}t\right) + \frac{c_3^1 - c_2^1\varsigma\beta}{\beta\sqrt{1-\varsigma^2}} e^{-\varsigma\beta t} \sin\left(\beta\sqrt{1-\varsigma^2}t\right) \\
& + c_4^1 \cos(2\pi\omega t) + \frac{c_5^1}{2\pi} \sin(2\pi\omega t) \Bigg],
\end{aligned}
$$

$$
\begin{aligned}
\eta_{60}(t) = \frac{1}{\delta_3} \Bigg[& c_1^2 + c_2^2 e^{-\lambda_1 t} + c_3^2 e^{-\varsigma\beta t} \cos\left(\beta\sqrt{1-\varsigma^2}t\right) + \frac{c_4^2 - c_3^2\varsigma\beta}{\beta\sqrt{1-\varsigma^2}} e^{-\varsigma\beta t} \sin\left(\beta\sqrt{1-\varsigma^2}t\right) \\
& + c_5^2 \cos(2\pi\omega t) + \frac{c_6^2}{2\pi} \sin(2\pi\omega t) \Bigg].
\end{aligned}
$$

(4.6)

We notice that the terms appearing in (4.6) and can be grouped into three parts: (i) constant term, indicating positional shift (only in yaw); (ii) oscillatory term, indicating harmonic behavior; and (iii) decay term. The terms having factors $e^{-\lambda_{i1} t}$ and $e^{-\varsigma\beta t}$ indicate damping and as $t \to \infty$, the effect of damping ceases to zero.

4.2. Numerical solution. Owing to the complexity in obtaining the analytical solution for higher-order equations involved in (4.2) and (4.3), we seek numerical solution and reduce the governing equations into a set of first-order equations with appropriate initial and boundary conditions,

$$
\dot{\eta}_4(t) = \phi_4, \qquad \dot{\eta}_6(t) = \phi_6,
$$

$$
\dot{\phi}_4 = \ddot{\eta}_4(t) = \frac{\left[F_4(t) - \{a_2(t)\dot{\eta}_4 + a_3(t)\eta_4 + b_1(t)\ddot{\eta}_6 + b_2(t)\dot{\eta}_6\}\right]}{a_1(t)},
$$

$$
\dot{\phi}_6 = \ddot{\eta}_6(t) = \frac{\left[F_6(t) - \{a_4(t)\ddot{\eta}_4 + a_5(t)\dot{\eta}_4 + b_4(t)\dot{\eta}_6\}\right]}{b_3(t)}.
$$

(4.7)

Table 5.1. Sectional coefficients of the floating body.

Wave	Sectional coefficients							
Frequency (dimensionless)	Sway added mass	Roll added mass	Sway-roll added mass	Sway damping	Roll damping	Sway-roll damping	Sway exciting force	Roll exciting moment
1.18	0.65	0.055	−0.13	1.0	0.02	−0.16	1.5	1.2

The system of (4.7) is solved by applying step-by-step integration procedure based on the Runge-Kutta-Gill method [24] with adaptive step-size adjustment algorithm to achieve desired accuracy. This scheme controls the growth of rounding errors efficiently and is stable with respect to the nonlinearity. The detailed description of model development and its validation are given in [23]. A computer program "SHIPMOT-RY-N" consisting of three main modules and several submodules is developed to implement detailed computational procedures of roll and yaw motions. These three main modules SHIP-D, SHIP-A, and SHIP-N deal with the relevant ship data, analytical, and numerical computations, respectively.

5. Numerical experiment and discussions

In order to perform numerical experiment, a vessel of length 150 m, beam 20.06 m, draught 9.88 m, and of mass 19 190 tons is considered. Further, we consider a sinusoidal wave of period 8.5 seconds (frequency 0.74 rad/s) with 1 m wave height and zero phase angle acting perpendicularly to the hull of the vessel. The sectional coefficients for added mass, damping, Froude-Krylov, and diffraction force are obtained (Table 5.1) on the basis of experimental study conducted by Vugts [25], and illustrated by Salvesen et al. [16].

It may be noticed that setting $b_1(t) = b_2(t) = a_4(t) = a_5(t) = 0$ in (2.11) and (2.12), uncoupled motion corresponding to roll and yaw can be derived. Prior to solving higher-order equations, we validate numerical scheme by comparing analytical solution with numerical solution for uncoupled zeroth-order roll motion and observed close agreement between them (Figure 5.1). We focus our analysis on damping sensitivity and the effects of exciting forces on uncoupled and coupled roll and yaw motions. It is apparent from (A.4) that the nonlinear forcing functions are having implicit dependence on angular motions; added mass and damping coefficients of roll and yaw. For simplification, we consider first- and second-order coefficients of virtual mass, a_{1i}, b_{1i}, a_{4i}, and b_{3i} $(i = 1, 2, \ldots)$ are in phase. The variations of roll and yaw amplitudes with frequency are plotted in Figures 5.2 and 5.3, and it is interesting to note that as frequency increases, roll amplitude decreases asymptotically whereas yaw decreases very fast while changing its direction to attain stationary state after a critical frequency $\omega_c = 100$. The nonlinearity in damping could be realized after analyzing the terms appearing in (3.3), which essentially consists of four parts: (i) damping due to the change in time-dependent virtual added mass; (ii) damping due to the product with linear angle; (iii) damping due to the product with quadratic angle; and (iv) damping due to viscous effect. The numerical contribution of each component showing first- and second-order approximations is plotted in
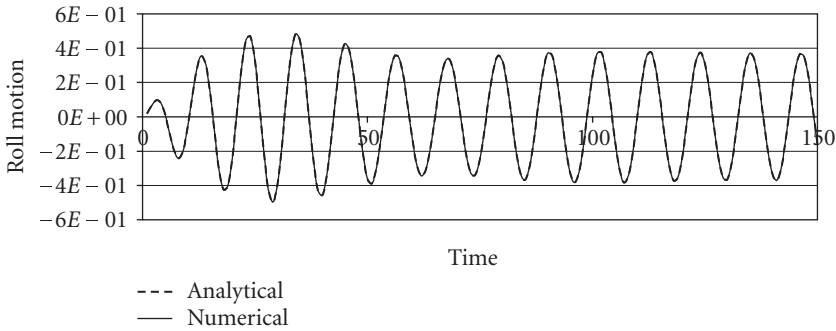
Figure 5.1. Comparison of analytical and numerical approaches for zeroth-order uncoupled roll motion.
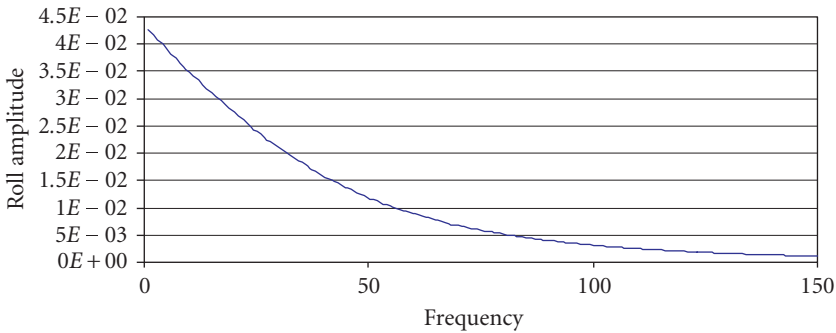

Figure 5.2. Variation of roll amplitude with frequency.

Figures 5.4–5.7, assigning the variable name as NLRDA (nonlinear roll-damping amplitude). We notice that the contribution due to change in added mass induces sinusoidal oscillation, whereas contribution from (ii), (iii), and (iv) shows decay with harmonic behavior as time increases. While accessing orderwise contributions, it may be noticed that the amplitude of viscous roll damping is dominant in comparison to other components for $t < 50$ seconds (Figure 5.7). Figure 5.8 shows combined contribution of orderwise roll damping. Using the above analysis, we access the contribution of first-order yaw damping and its components NLYDA (nonlinear yaw damping amplitude), and notice the dominance of yaw added mass variation over viscous and other damping terms in contrast to roll damping (Figures 5.9 and 5.10). However, the magnitudes of yaw damping terms are smaller than the corresponding roll-damping counterpart (Figures 5.8 and 5.11). In foregoing analysis, the all damping terms appear to be very small due to dimensionless formulation with respect to constant reference added mass coefficient $a_0 \approx O(10^7)$. In spite of having nonlinear dependence on angular motions, added mass and damping coefficients, the forcing moments manifest harmonic oscillations (Figures 5.12 and 5.13).
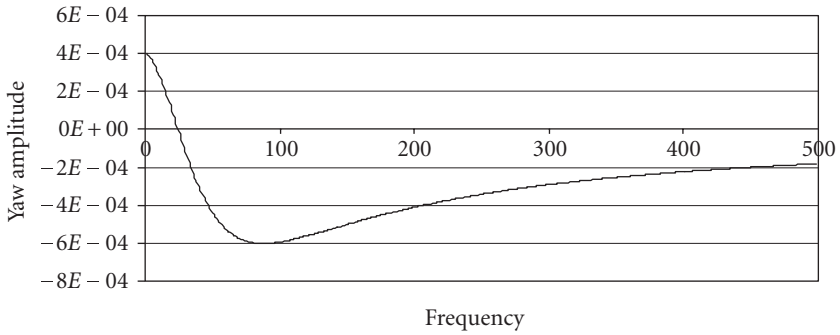
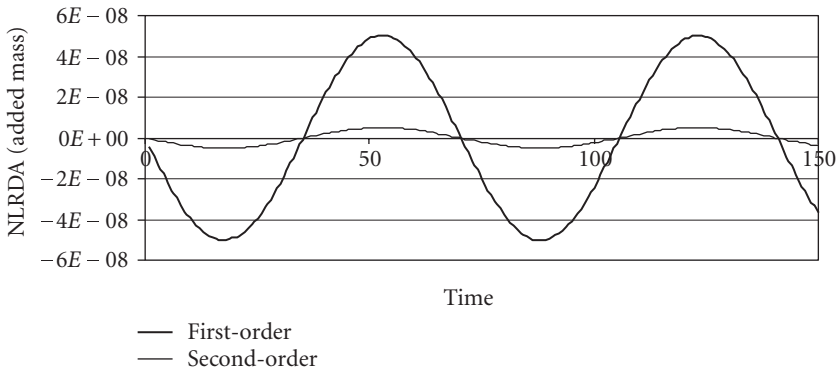Figure 5.3. Variation of yaw amplitude with frequency.

—— First-order
—— Second-order

Figure 5.4. Contribution of first- and second-order roll damping.
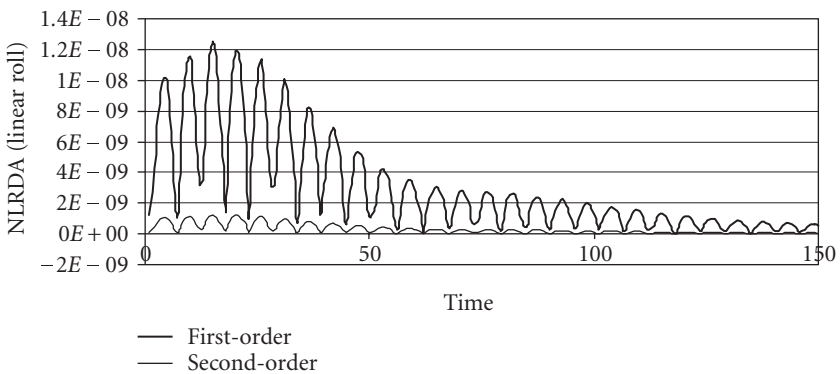

—— First-order
—— Second-order

Figure 5.5. Comparison of linear roll damping: first-order versus second-order.

We access the effect of coupling for zeroth-order case where closed-form solution reveals higher roll amplitudes with phase lag for uncoupled case (Figure 5.14). The reduction in degrees of freedom from two to one enhances phase lag and exhibits artificial
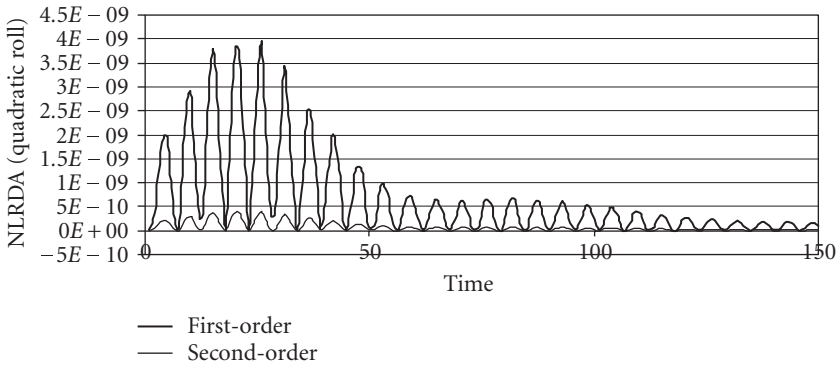
Figure 5.6. Comparison of quadratic roll damping: first-order versus second-order.

Figure 5.7. Comparison of viscous roll damping: first-order versus second-order.

Figure 5.8. Comparison of combined roll damping: first-order versus second-order.

increase in amplitude due to the imbalance caused in the absence of yaw (Figure 5.14). This is also apparent from Table 5.2 where the effects of NLRDA are shown while comparing the nonlinear roll damping (after 125 seconds) for coupled and uncoupled cases.

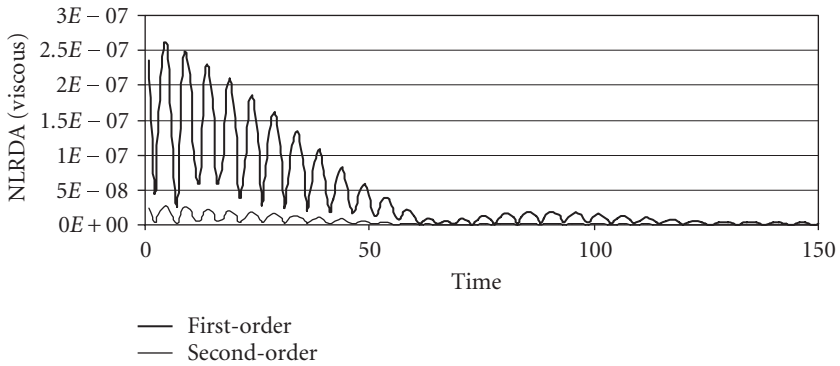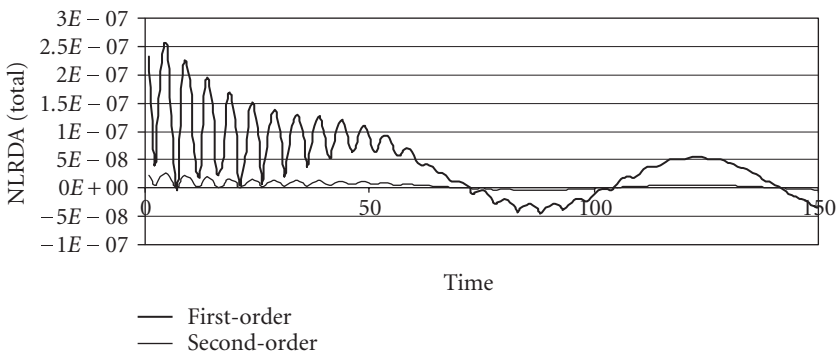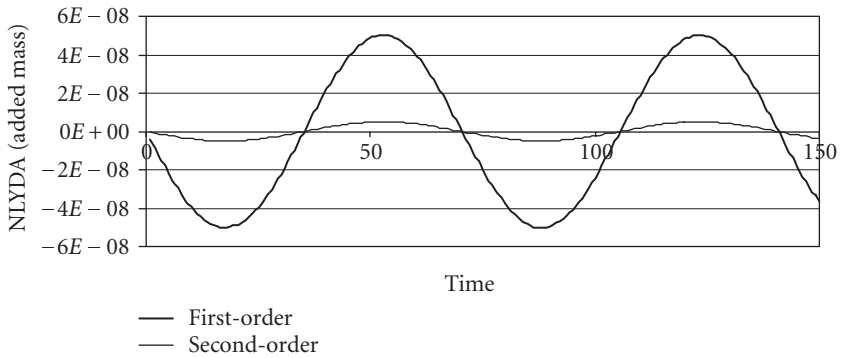Figure 5.9. Comparison of yaw damping amplitudes due to variation of added mass: first-order versus second-order.
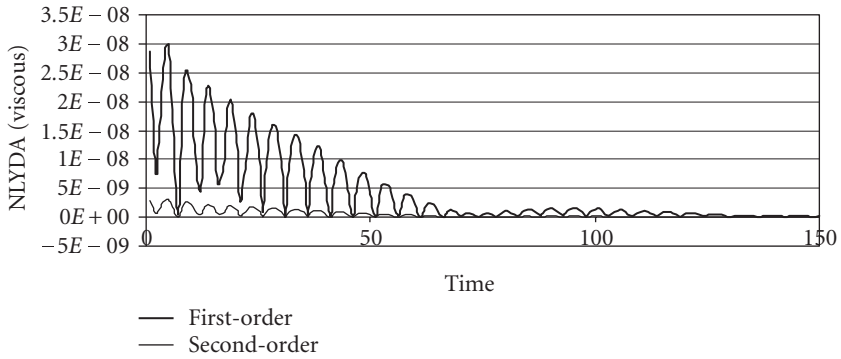
Figure 5.10. Comparison of viscous yaw damping: first-order versus second-order.
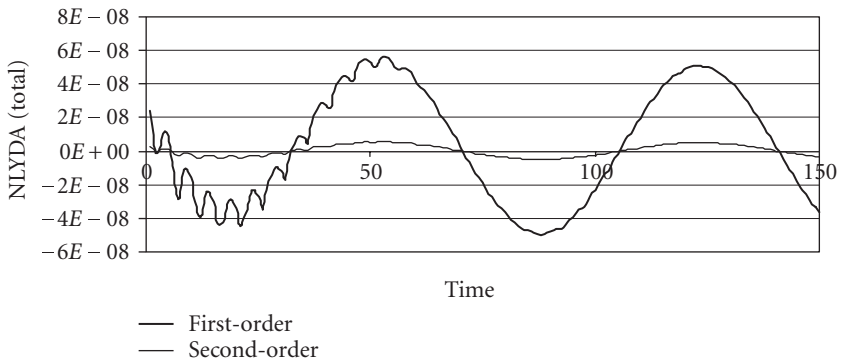
Figure 5.11. Comparison of yaw damping: first-order versus second-order.

However, the amplitudes of coupled yaw motion are found to be greater than the corresponding amplitude of uncoupled yaw motion except in first-order case as shown in
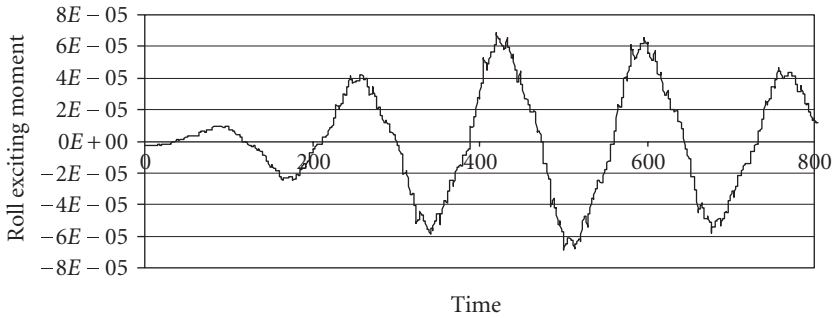
Figure 5.12. First-order wave forcing function on roll.
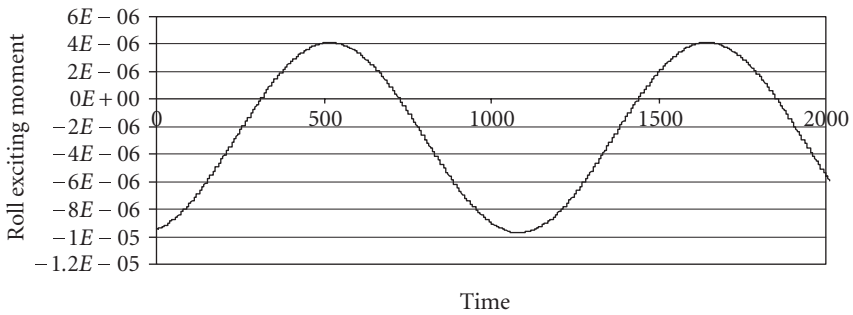
Figure 5.13. Second-order wave forcing function on roll.
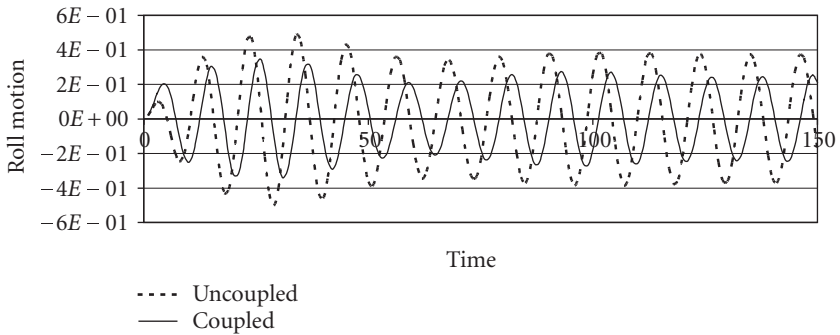
- - - - Uncoupled
——— Coupled

Figure 5.14. Comparison of zeroth-order roll motion solved analytically: uncoupled against coupled motions.

Table 5.3 (NLYDA). Figure 5.15 shows significant increase in oscillations in yaw angle for zeroth-order coupled motion in contrast to the uncoupled one when solved analytically.

6. Conclusion

We have presented analytical and computational approaches to study the nonlinear dependence of added mass and damping for roll and yaw motions while external wave force

Figure 5.15. Comparison of zeroth-order yaw motions solved analytically: uncoupled against coupled motions.

Table 5.2. Contribution of nonlinear roll damping after 125 seconds (NLRDA).

Uncoupled roll motion			Coupled roll motion		
Zeroth order	First order	Second order	Zeroth order	First order	Second order
$\pm 4.0 \times 10^{-1}$	$\pm 1.0 \times 10^{-6}$	-1.3×10^{-7}	$\pm 2.0 \times 10^{-1}$	$\pm 5.0 \times 10^{-8}$	$\pm 5.0 \times 10^{-9}$

Table 5.3. Contribution of nonlinear yaw damping after 125 seconds (NLYDA).

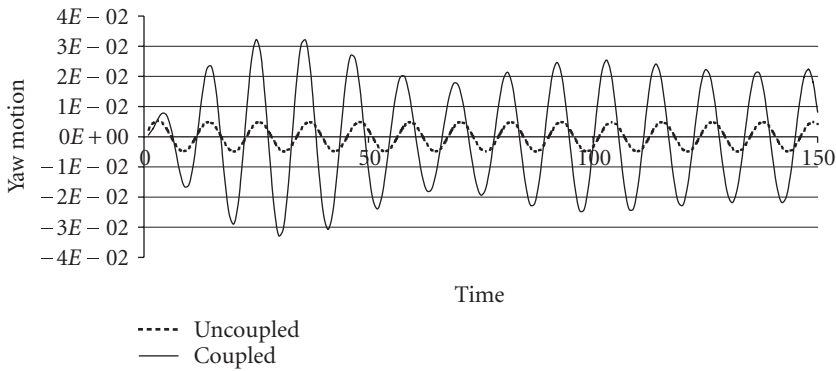| Uncoupled yaw motion			Coupled yaw motion		
Zeroth order	First order	Second order	Zeroth order	First order	Second order
$\pm 8.0 \times 10^{-3}$	$\pm 5.0 \times 10^{-8}$	$\pm 1.0 \times 10^{-9}$	$\pm 2.0 \times 10^{-2}$	$\pm 5.0 \times 10^{-8}$	$\pm 4.0 \times 10^{-9}$

is harmonic. Using the perturbation analysis, we are able to access the nonlinear form and implicit functional dependence of angular motions in added mass and damping coefficients. Using these theoretical and computational techniques, one can also estimate the system stability, damping, and their interrelationship for a known wave frequency. The finding of the model result shows that the viscous effect becomes significant for roll damping; whereas for yaw damping, the effect of added mass becomes significant.

Appendix

Expressions for dimensionless quantities appeared in (2.11) and (2.12),

$$\bar{\eta}_4 = \frac{\eta_4}{\eta_0}, \qquad \bar{\eta}_6 = \frac{\eta_6}{\eta_0}, \qquad \bar{a}_1(t) = \frac{[I_4 + A_{44}(t)]}{a_0}, \qquad \bar{a}_2(t) = \frac{B_{44}(t)t_0}{a_0},$$

$$\bar{a}_3(t) = \frac{C_{44}(t)t_0^2}{a_0}, \qquad \bar{a}_4(t) = \frac{[-I_{46} + A_{64}(t)]}{a_0}, \qquad \bar{a}_5(t) = \frac{B_{64}(t)t_0}{a_0},$$

$$\overline{b}_1(t) = \frac{\left[-I_{46} + A_{64}(t)\right]}{a_0}, \quad \overline{b}_2(t) = \frac{B_{46}(t)t_0}{a_0}, \quad \overline{b}_3(t) = \frac{\left[I_6 + A_{66}(t)\right]}{a_0},$$

$$\overline{b}_4(t) = \frac{B_{66}(t)t_0}{a_0}, \quad \overline{F}_4(t) = \frac{F_4(t)t_0^2}{a_0\eta_0}, \quad \overline{F}_6(t) = \frac{F_6(t)t_0^2}{a_0\eta_0}, \quad \overline{\omega} = \frac{\omega_e}{\omega_0}, \quad \text{(A.1)}$$

where a_0 is the reference virtual mass moment of inertia and ω_0 is reference frequency corresponding to the wave periodicity t_0 seconds.

The detailed expressions for a_{1i}, b_{1i}, a_{4i}, and b_{3i} appeared in (3.2),

$$a_{1i}(t) = \sigma\cos(\omega t), \quad i = 1,2,\dots, \quad b_{1i}(t) = \sigma\cos(\omega t), \quad i = 1,2,\dots,$$

$$a_{4i}(t) = \sigma\cos(\omega t), \quad i = 1,2,\dots, \quad b_{3i}(t) = \sigma\cos(\omega t), \quad i = 1,2,\dots. \quad \text{(A.2)}$$

The detailed expressions for a_{2i}, b_{2i}, a_{5i}, and b_{4i} appeared in (3.4),

$$a_{2i}(t) = \sigma e^{-\varsigma\beta t}, \quad i = 1,2,\dots, \quad b_{2i}(t) = \sigma e^{-\varsigma\beta t}, \quad i = 1,2,\dots, \quad \sigma = \frac{1}{a_0},$$

$$a_{5i}(t) = \sigma e^{-\varsigma\beta t}, \quad i = 1,2,\dots, \quad b_{4i}(t) = \sigma e^{-\varsigma\beta t}, \quad i = 1,2,\dots. \quad \text{(A.3)}$$

Expressions for $F_4^i(t)$ and $F_6^i(t)$, $i = 1,2$, appeared in (4.2) and (4.3),

$$F_4^0(t) = F_4^{a0}\sin(\omega t + \theta), \qquad F_6^0(t) = F_6^{a0}\sin(\omega t + \theta),$$

$$F_4^1(t) = -\left[a_{11}(t)\ddot{\eta}_{40}(t) + \left\{a_{21}(t)\left|\eta_{40}(t)\right| + a_{22}(t)\eta_{40}^2(t) + a_{23}(t)\left|\dot{\eta}_{40}(t)\right|\right\}\dot{\eta}_{40}(t)\right]$$

$$\qquad - \left[b_{11}(t)\ddot{\eta}_{60}(t) + \left\{b_{21}(t)\left|\eta_{60}(t)\right| + b_{22}(t)\eta_{60}^2(t) + b_{23}(t)\left|\dot{\eta}_{60}(t)\right|\right\}\dot{\eta}_{60}(t)\right],$$

$$F_6^1(t) = -\left[a_{41}(t)\ddot{\eta}_{40}(t) + \left\{a_{51}(t)\left|\eta_{40}(t)\right| + a_{52}(t)\eta_{40}^2(t) + a_{53}(t)\left|\dot{\eta}_{40}(t)\right|\right\}\dot{\eta}_{40}(t)\right]$$

$$\qquad - \left[b_{31}(t)\ddot{\eta}_{60}(t) + \left\{b_{41}(t)\left|\eta_{60}(t)\right| + b_{42}(t)\eta_{60}^2(t) + b_{43}(t)\left|\dot{\eta}_{60}(t)\right|\right\}\dot{\eta}_{60}(t)\right],$$

$$F_4^2(t) = -\left[a_{12}(t)\ddot{\eta}_{40}(t) + \left\{\dot{a}_{11}(t) + a_{24}(t)\left|\eta_{40}(t)\right| + a_{21}(t)\left|\eta_{41}(t)\right| + 2a_{22}(t)\eta_{40}(t)\eta_{41}(t)\right.\right.$$

$$\qquad \left.\left. + a_{25}(t)\eta_{40}^2(t) + a_{26}(t)\left|\dot{\eta}_{40}(t)\right| + a_{23}(t)\left|\dot{\eta}_{41}(t)\right|\right\}\dot{\eta}_{40}(t)\right]$$

$$\qquad - \left[a_{11}(t)\ddot{\eta}_{41}(t) + \left\{a_{21}(t)\left|\eta_{40}(t)\right| + a_{22}(t)\eta_{40}^2(t) + a_{23}(t)\left|\dot{\eta}_{40}(t)\right|\right\}\dot{\eta}_{41}(t)\right]$$

$$\qquad - \left[b_{12}(t)\ddot{\eta}_{60}(t) + \left\{\dot{b}_{11}(t) + b_{24}(t)\left|\eta_{60}(t)\right| + b_{21}(t)\left|\eta_{61}(t)\right| + 2b_{22}(t)\eta_{60}(t)\eta_{61}(t)\right.\right.$$

$$\qquad \left.\left. + b_{25}(t)\eta_{60}^2(t) + b_{26}(t)\left|\dot{\eta}_{60}(t)\right| + b_{23}(t)\left|\dot{\eta}_{61}(t)\right|\right\}\dot{\eta}_{60}(t)\right]$$

$$\qquad - \left[b_{11}(t)\ddot{\eta}_{61}(t) + \left\{b_{21}(t)\left|\eta_{60}(t)\right| + b_{22}(t)\eta_{60}^2(t) + b_{23}(t)\left|\dot{\eta}_{60}(t)\right|\right\}\dot{\eta}_{61}(t)\right],$$

$$F_6^2(t) = -\left[a_{42}(t)\ddot{\eta}_{40}(t) + \left\{\dot{a}_{41}(t) + a_{54}(t)\left|\eta_{40}(t)\right| + a_{51}(t)\left|\eta_{41}(t)\right| + 2a_{52}(t)\eta_{40}(t)\eta_{41}(t)\right.\right.$$

$$\qquad \left.\left. + a_{55}(t)\eta_{40}^2(t) + a_{56}(t)\left|\dot{\eta}_{40}(t)\right| + a_{53}(t)\left|\dot{\eta}_{41}(t)\right|\right\}\dot{\eta}_{40}(t)\right]$$

$$\qquad - \left[a_{41}(t)\ddot{\eta}_{41}(t) + \left\{a_{51}(t)\left|\eta_{40}(t)\right| + a_{52}(t)\eta_{40}^2(t) + a_{53}(t)\left|\dot{\eta}_{40}(t)\right|\right\}\dot{\eta}_{41}(t)\right]$$

$$\qquad - \left[b_{32}(t)\ddot{\eta}_{60}(t) + \left\{\dot{b}_{31}(t) + b_{44}(t)\left|\eta_{60}(t)\right| + b_{41}(t)\left|\eta_{61}(t)\right| + 2b_{42}(t)\eta_{60}(t)\eta_{61}(t)\right.\right.$$

$$\qquad \left.\left. + b_{45}(t)\eta_{60}^2(t) + b_{46}(t)\left|\dot{\eta}_{60}(t)\right| + b_{43}(t)\left|\dot{\eta}_{61}(t)\right|\right\}\dot{\eta}_{60}(t)\right]$$

$$\qquad - \left[b_{31}(t)\ddot{\eta}_{61}(t) + \left\{b_{41}(t)\left|\eta_{60}(t)\right| + b_{42}(t)\eta_{60}^2(t) + b_{43}(t)\left|\dot{\eta}_{60}(t)\right|\right\}\dot{\eta}_{61}(t)\right]. \quad \text{(A.4)}$$

References

[1] W. Froude, "On the rolling of ships," *Institution of Naval Architects Transactions*, vol. 2, pp. 180–229, 1861.

[2] J. E. Kerwin, "Notes on rolling in longitudinal waves," *International Shipbuilding Progress*, vol. 2, pp. 597–614, 1955.

[3] M. R. Haddara, "On the stability of ship motion in regular oblique waves," *International Shipbuilding Progress*, vol. 18, no. 207, pp. 416–434, 1971.

[4] J. F. Dalzell, "Note on the form of ship roll damping," *Journal of Ship Research*, vol. 22, no. 3, pp. 178–185, 1978.

[5] M. R. Haddara, "A note on the effect of damping moment form on rolling response," *International Shipbuilding Progress*, vol. 31, no. 363, pp. 285–290, 1984.

[6] A. H. Nayfeh and A. A. Khdeir, "Nonlinear rolling of ships in regular beam seas," *International Shipbuilding Progress*, vol. 33, no. 379, pp. 40–49, 1986.

[7] A. Cardo, A. Francescutto, and R. Nabergoj, "On damping models in free and forced rolling motion," *Ocean Engineering*, vol. 9, no. 2, pp. 171–179, 1982.

[8] J. B. Mathisen and W. G. Price, "Estimation of ship roll damping coefficients," *Royal Institution of Naval Architects Transactions*, vol. 127, pp. 169–186, 1985.

[9] J. R. Spouge, "Nonlinear analysis of large-amplitude rolling experiments," *International Shipbuilding Progress*, vol. 35, no. 403, pp. 271–320, 1988.

[10] J. B. Roberts, "Estimation of nonlinear ship roll damping from free-decay data," *Journal of Ship Research*, vol. 29, no. 2, pp. 127–138, 1985.

[11] D. W. Bass and M. R. Haddara, "Nonlinear models of ship roll damping," *International Shipbuilding Progress*, vol. 35, no. 401, pp. 5–24, 1988.

[12] M. R. Haddara and P. Bennett, "A study of the angle dependence of roll damping moment," *Ocean Engineering*, vol. 16, no. 4, pp. 411–427, 1989.

[13] M. R. Haddara and D. W. Bass, "On the form of roll damping moment for small fishing vessels," *Ocean Engineering*, vol. 17, no. 6, pp. 525–539, 1990.

[14] H. H. Chun, S. H. Chun, and S. Y. Kim, "Roll damping characteristics of a small fishing vessel with a central wing," *Ocean Engineering*, vol. 28, no. 12, pp. 1601–1619, 2001.

[15] S. N. Das and S. K. Das, "Determination of coupled sway, roll, and yaw motions of a floating body in regular waves," *International Journal of Mathematics and Mathematical Sciences*, vol. 2004, no. 41, pp. 2181–2197, 2004.

[16] N. Salvesen, E. O. Tuck, and O. M. Faltinsen, "Ship motions and sea loads," *Transactions of Society of Naval Architects and Marine Engineers*, vol. 78, pp. 250–287, 1970.

[17] L. J. Tick, "Differential equations with frequency-dependent coefficients," *Journal of Ship Research*, vol. 3, no. 2, pp. 45–47, 1959.

[18] W. E. Cummins, "The impulse response function and ship motions," *Schiffstechnik*, vol. 9, pp. 101–109, 1962.

[19] J. P. Hooft, *Advanced Dynamics of Marine Structures*, John Willey & Sons, New York, NY, USA, 1982.

[20] M. Söylemez, "Motion response simulation of a twin-hulled semi-submersible," *Ocean Engineering*, vol. 25, no. 4-5, pp. 359–383, 1998.

[21] J. R. Spouge, N. Ireland, and J. P. Collins, "Large amplitude rolling experiment techniques," in *Proceedings of International Conference on Stability of Ships and Ocean Vehicles*, Gdansk, Poland, 1986.

[22] A. H. Nayfeh, *Perturbation Methods*, John Wiley & Sons, New York, NY, USA, 1981.

[23] S. N. Das and S. K. Das, "Mathematical model for coupled roll and yaw motions of a float-
      ing body in regular waves under resonant and non-resonant conditions," *Applied Mathematical
      Modelling*, vol. 29, no. 1, pp. 19–34, 2005.

[24] W. H. Press, S. A. Teukalsky, W. T. Vetterling, and B. P. Flannery, *Numerical recipes in FORTRAN*,
      Cambridge University Press, Cambridge, UK, 2nd edition, 1992.

[25] J. H. Vugts, "The hydrodynamic coefficients for swaying, heaving and rolling cylinders in a free
      surface," Tech. Rep. 194, Laboratorium voor Scheepsbouwkunde, Technische Hogeschool, Delft,
      Netherlands, 1968.

S. K. Das: CFD-AIT Program, International Institute of Information Technology (I2IT),
P-14 Pune Infotech Park, Hinjewadi, Pune 411 057, India
Email addresses: samird@isquareit.ac.in ; samirkumar_d@yahoo.com

S. N. Das: Central Water and Power Research Station, Khadakwasla, Pune 411 024, India
Email address: sndas_cwprs@rediffmail.com

Advances in
Operations Research

Advances in
Decision Sciences

Journal of
Applied Mathematics

Algebra

Journal of
Probability and Statistics

The Scientific
World Journal

International Journal of
Differential Equations

International Journal of
Combinatorics

Advances in
Mathematical Physics

Journal of
Complex Analysis

Journal of
Mathematics

Mathematical Problems
in Engineering

Abstract and
Applied Analysis

Discrete Dynamics in
Nature and Society

International
Journal of
Mathematics and
Mathematical
Sciences

Journal of
Discrete Mathematics

Journal of
Function Spaces

International Journal of
Stochastic Analysis

Journal of
Optimization